Implementation of Gravity Investigations across Aqra Structures - Iraq

Marwan Mutib[1]*, Maan H Al-majid[2] and Fadhil A Ghaib[3]

[1]Department of Mining Engineering, College of Petroleum and Mining Engineering, University of Mosul, Iraq
[2]Department of Petroleum Reservoir Engineering, College of Petroleum and Mining Engineering, University of Mosul, Iraq
[3]Department of Geology, College of Science, University of Salah Al-din, Iraq

ABSTRACT

The surveyed area covering about 2000 km2 in the north-eastern Iraq with elevations ranges between 300 to 1900 m above sea level. The study area is located within the foot hill and high folded zones including a number of important anticlines (Aqra, Piris, Barat, and else). The geophysical survey is based on 170 gravity points. The gravity data had been corrected and the Bouguer anomaly was calculated along each point. The 2D modeling technique by using Geosoft Oasis Montaj program was applied for the quantitative interpretation. Six gravity profiles were modelled. The results of this study show that the top depth of the basements rocks in the studied area is around 9 km, and several faults are indicated in the sedimentary sections by gravity profiles. The results of the modelled profiles are identified that the several grabens, half grabens and horsts surrounded by normal and reverse faults are displayed in the sedimentary sections by gravity "lows" and "highs"

INTRODUCTION

Gravity methods are effectively used in basic geological, geothermal studies and engineering applications. More importantly, the nature of the gravity methods allows a reciprocal benefit with the seismic method: gravimetric inversion profits from constraints provided by the seismic data by helping to minimize the number of possible solutions, and gravity can aid with the imaging in areas in which the seismic method is less effective, such as in subsalt areas or crystalline environments. The gravity anomalies are resulted from lateral variations in the density of subsurface materials and the distance to these bodies from the measuring points. The gravity method is one of the best ways to discover the subsurface structures and recognize the variations in the thickness of sedimentary cover so it has been used in this study. This study includes the analysis of gravity data to delineate and locate any structures and faults in the study area. The area of study covers about 2000 km² around the Aqra region bounded by longitudes 43° 59` E - 44° 36` E and latitudes 36° 49` N – 36°92` N. There are a number of anticlines on the study area (Aqra, Piris, and else) [1-5]

Iraq was divided into three tectonically different areas, the Stable Shelf with major buried arches and antiforms but no surface anticlines; the Unstable Shelf with surface anticlines, and Zagros Suture which comprises thrust sheets of radiolarian chert, igneous and metamorphic rocks (Figure 1). The study area is a part of the Foreland folds of the Alpine Orogen in northern Iraq, and they are located on the Mosul block that trend in a Taurus E-W direction [6,7].

The stratigraphy underneath the study area plains is inferred from the outcrops of anticlines bounded these plains (Figure 2). The elevation of this area ranges between 300m (at the south Aqra region) to 1900 m (at the north-eastern of the study area).

Geophysical data are few for the north-eastern parts of Iraq except some local surveys around Erbil area. The Bouguer anomaly map of Iraq, did not cover the northern parts. The gravity review made also revealed lack of data in those parts of Iraq [8-10].

Estimate of the local and regional seismic velocity structures of north and north-eastern Iraq included the northern extension of the Zagros collision zone using well-established seismological techniques. Preliminary results indicated that the depth of the Moho varies considerably beneath North Iraq Seismographic Network. It is relatively shallow 35-45 km to the northwest and deeper 50-60 km under the south-eastern portion of the network area [11].

Estimate thickness of the sedimentary cover overlying the basement

---

*Corresponding author: Mutib M, Department of Mining Engineering, College of Petroleum and Mining Engineering, University of Mosul, Iraq, Tel: 07701835443; E-mail: drmarwanmutib@yahoo.com
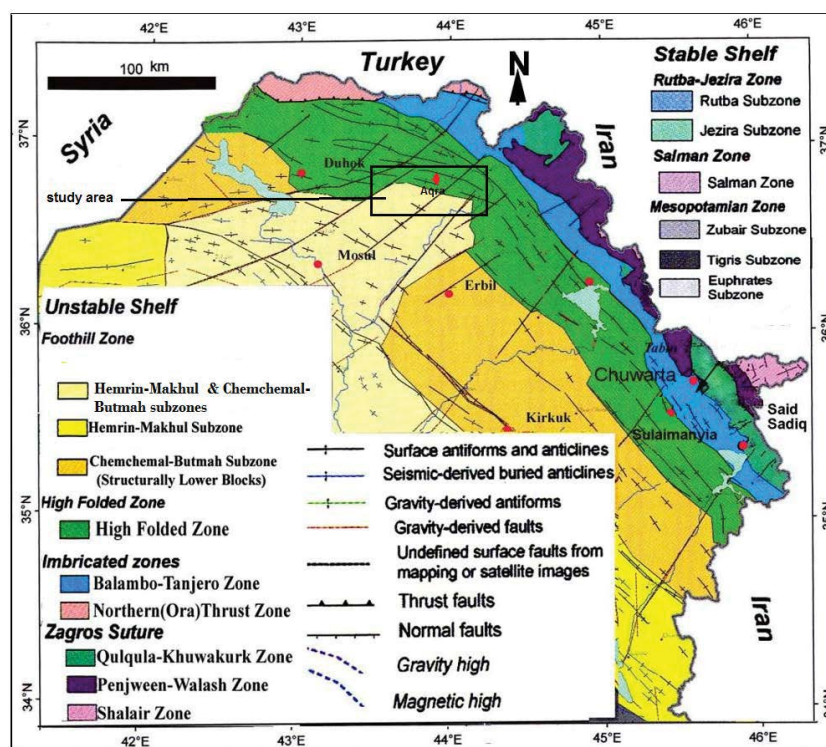
Figure 1: Tectonic zones and structural elements of unstable shelf [6] with locations of study area.
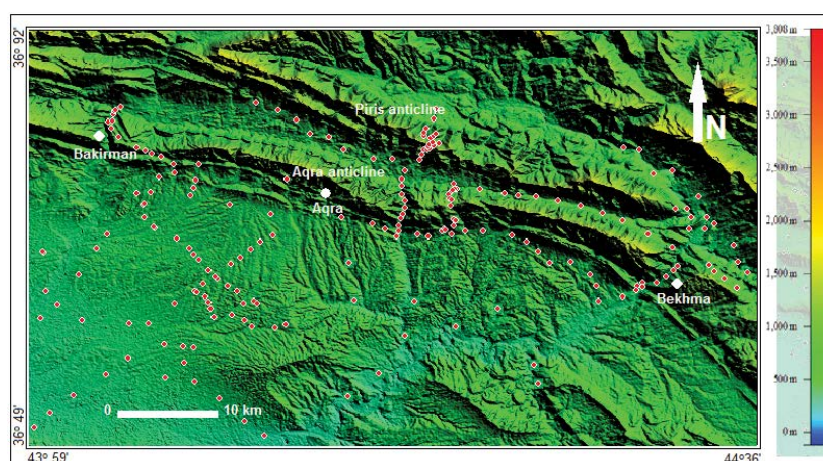
Figure 2: The location of the study area on the Digital Elevation Model (DEM) showing geomorphologic features and the locations of gravity stations (Red dots).

complex in Aqra area, i.e., the depth to the basement is calculated from the gravity data using two best approximation alternative density contrast between the sedimentary and basement. A density contrast of 0.13 gm/cm³ puts the depth of the basement 9-10 km while a contrast of 0.18 g/cm³ gives a depth of 5.5-6 km. The depths given by the contrast of 0.13 g/cm³ seem more realistic. Regional and local profiles in the Aqra area show that the distinctive density contrast is present within the stratigraphic succession between the Upper Cretaceous formations (2.57 g/cm³) and the Paleogene formations 2.28 g/cm³ Ghaib (op.cit.) pointed out the existing of the Malabarwan fault in the Aqra area in both the gravity and magnetic data implying that these subsurface faults penetrate deep into the basement rocks applied seventy three gravity and magnetic measurements along two traverses cutting the Greater Zab River in two different areas. Their study aims to throw light on the subsurface geological picture. Gravity data have proven to be useful for modelling the basement undulation in settings where it is covered by thick sedimentary successions [12-14].

In gravity survey, the variations in the earth's gravitational field were caused by differences in the density of subsurface rocks. The determination of the density contrast between basement rocks and the sedimentary cover is essential in estimating the basement depth by the gravimetric method. Most of the authors have used the value 0.17 g/cm³ as a density contrast between sedimentary cover and basement rocks as reviewed. In Demir dagh area estimated the density contrast between crystalline basement and overlying sedimentary cover to be 0.16 g/cm³. Assuming such contrast, the basement was calculated to be at a depth of about 10 km. Nevertheless, used the value 0.18 gm/cm³ in a regional traverse along and around the present study areas. This value is by who recommended its use in the Unstable Shelf of Iraq. The mean density of the sedimentary cover was given to be 2.6 gm/cm³ considering an average density of 2.77 g/cm³ for the basement rocks developed a schedule of the formations in his study area (nearby this study area) showing their thicknesses, ages and lithology [9,15-19].

Since there is no gravity investigation carried out for the study

area with exception of some local studies, so the present work is intended to a complement of the gap in this area.

MATERIAL AND METHODS

LaCoste and Romberge Gravimeter model G was used in this study. It has a range of more than 700 milligals, reading accuracy of ± 0.01 mgl and a drift of less than 1 mgl/month. When this gravimeter was calibrated before the field work, the calibration factor did not change perceptibly with time. This eliminated the need for frequent checks of calibration during the work. The instrument did not show troubles during the period of work.

In this work, all gravity stations were surveyed for relative easting, northing, and elevation using a Garmin 72 Global Positioning System (GPS). The elevation of the reading station, relative to sea level shows accuracy ± 4 m when it is used continuously in the field. A Garmin 72 GPS has not exceeded few meters for coordinates accuracy horizontally.

The primary base station is known as absolute gravity and elevation station, it is located in the Mosul University from [20]. This station has an absolute value of 979789.46 mGal which is used as a reference point for the other stations in the studied area. The absolute value of the gravity could be found for those stations from the absolute value of the primary base station. In addition, eight secondary base stations were established in the studied area and tied with primary base station. Transportation of the gravimeter from the base station to other stations and from one station to another was the most time consuming aspect.

The form of the field work means the way of the stations array, which is common by these ways: traverses, gird and random way. In this study the random way is used for arraying the stations due to the major difficulties (mountains & valleys) in the study area. To facilitate the survey, it is a common practice to establish 170 gravity stations near and along highways, roads and their branches depending upon feasibility of access and the spacing pattern necessary to detail the features (Figure 2).

Single-base method (the gravity base station) was adopted to correct the gravity readings in every station for the effect of temperature and pressure (Figure 3).

The Bouguer anomaly of the gravity at a point is the difference between the observed value ($g_{obs.}$) adjusted by the algebraic sum of all the necessary corrections ($\sum$corr.) and that at base station

$$(g_{base}): \Delta g_B = g_{obs} + \sum corr. - g_{base} \tag{1}$$

$$\Delta g_B = (g_{abs.} - g_{theo.}) + (0.3086 - 0.04193\rho)h + \Delta g_{Ter.} \tag{2}$$

where h is the elevation above sea level, gabs is the absolute gravity value in the measurement point. This implies a known absolute value at the base station and g_{theo} is the theoretical gravity value at the geographic station latitude (φ) at sea level.

The theoretical gravity value which is usually denoted by (g_φ) varies over the surface of the earth because of its ellipsoidal shape. The International Association of Geodesy (IAG) in 1971 proposed a formula to calculate g_φ at any latitude:

$$g_\phi = 9.780318(1 + 0.0053024\sin^2\phi - 0.0000059\sin^2 2\phi)m/s^2 \tag{3}$$

This formula gives the actual gravity value at sea level to within 0.1 mgl precision. This formula is applied in the present work. It is important to mention here, that the Iraqi gravity surveys (the IPC – Bouguer map and later surveys) had applied the 1930's formula which differs by about 12.5 milligals from the 1971's formula [12].

$$g_\phi = 9.78049(1 + 0.0052884\sin^2\phi - 0.0000059\sin^2 2\phi)m/s^2 \tag{4}$$

In an environment of irregular topography, the undulations above and below the elevation level of gravity observations are referred to as terrain correction to as terrain correction. Terrain correction is necessary when the gravity effect due to topography between any station and the base station level is over the accuracy of gravimeter. Computing these corrections by hand using topographic maps is a labor intensive task. As noted by Hammer's method is manual, tedious and prone to estimation error [21].

Efficient and effective use of these corrections requires comprehensive (DEM) and computational power that is only now becoming generally available [22-24]

For each elevation point within the 30 meter DEM image compared to the elevation of the gravity station is calculated. A rectangular prism with uniform density 2.175 g/cm³ is used to calculate the vertical component of the gravitational attraction between the gravity station and the prism. The Geosoft Oasis Montaj program set [25] and Terrain Correction Software (TCS) extension provides
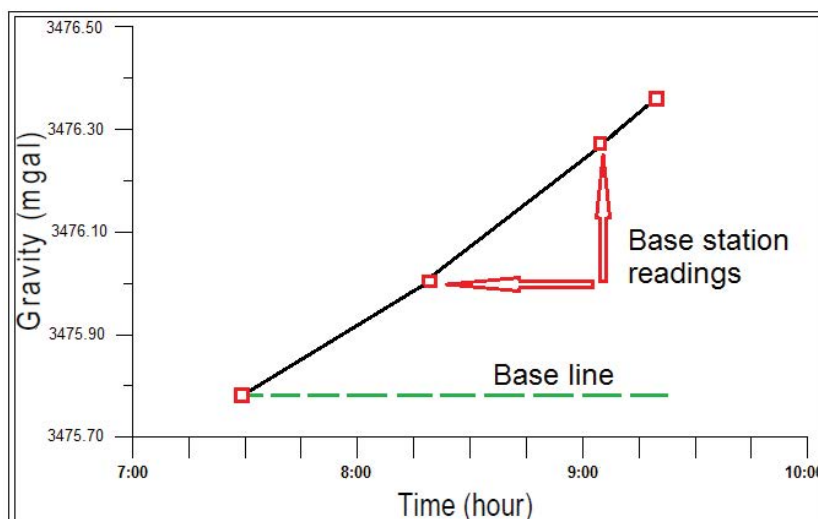
Figure 3: Drift curve for one-day gravity work 07/08/2010

a complete system for processing and reducing gravity data from conventional ground surveys.

The data obtained after application of the reduction on the raw data may be affected by several errors; the first is produced by the instrument itself and the second by field and reduction procedures.

Instrumental errors come from the inaccurate reading of the data. Repeated readings in 61 stations showed an error in the observation of ± 0.04 mGal in (Δg_o). The second type of errors affects the gravity values more seriously. The errors encountered in this study are listed in Table 1. The total error in the Bouguer anomaly can be calculated using this formula:

$$E_{total} = \sqrt{E^2 g_0 + E^2_{Fa} + E2_{Bc} + E^2_{lat.}} = \pm\ 1.29\ \text{mgl} \qquad (5)$$

The methods used to calculate the gravity model response are based on the methods of [26,27] and make use of the algorithms [28]. The GM-SYS inversion routine utilizes an inversion algorithm to linearize and invert the calculations. GM-SYS uses an implementation of that algorithm for gravity developed by the USGS and used in their computer program [29-31]. GM-SYS uses a two-dimensional, flat-earth model for the gravity calculations; that is, each structural unit or block extends to plus and minus infinity in the direction perpendicular to the profile. The earth is assumed

to have topography but no curvature. The model also extends plus and minus 30,000 km along the profile to eliminate edge effects. The modelling software according to Talwani M [25] was calculated for each survey line using all gravity station locations. All station distances were calculated from the first station on each line (always the southernmost station).

For both the preliminary estimations and the final calculations, the density of different rock units of the causative bodies and the surroundings should be known as precisely as possible in order to calculate the density contrast which is the cause of the gravity anomalies. All previous lithostratigraphic and structural studies were also taken into account to produce the models (Table 2) describes the modelled units used in all modelled profiles of the present study.

RESULTS

The first step in the quantity interpretation is the visual inspection of the residual map to choose the profile across the anomaly of interest. The second is to estimate approximately the horizontal extension, depth, shape and thickness of target using a geological background (Well logging, seismic sections and previous studies). The third step is to construct a geometric model which satisfies the above mentioned estimations and is consistent with the geologic situation by using recent computer programming [25].

The derivation of regional and residual components of the gravity field through wavelength filtering is accomplished through the association of a specific range of wavelengths with different source depths. There are a number of methods can be applied to isolate the residual anomaly from the regional anomaly were reviewed by a number of investigators [32]. The separation of residual anomaly in this study is performed by using the empirical method [33]. The optimum upward continuation height was determined by calculating correlation factor r between upward continuation fields at two successive heights. The correlation factor is plotted as a function of increasing continuation height. The height increases from zero to a level where the change in correlation values has clearly passed the point giving rise to a maximum deflection. The height that gives the maximum deflection is the optimum height (Figure 4).

The designed models include the sedimentary sequence and the basement complex with the structure situation, and the thickness

Table 1: Source and magnitudinal effects of errors.

Source	Magnitudinal Effect (mGl)
Measurement error (go)	0.04
Elevation (Free air) error (Fa)	1.23
Elevation (Bouguer) error (Bc) including density	0.38
Latitude error (lat)	0.02
Terrain elevation error(Tc) + Density error	0.0006 + 0.15

Table 2: Describes the modeled units and their densities.

Geologic period	Density (g/cc)	Reference
Quaternary and Neogen	2.175	[8, 29]
Paleogen	2.33	Calculated form [15, 12]
Cretaceous	2.57	[12]
Jorassic and Triasic	2.71	[30]
Paleozoic	2.65	[30]
Basement	2.78	[18]
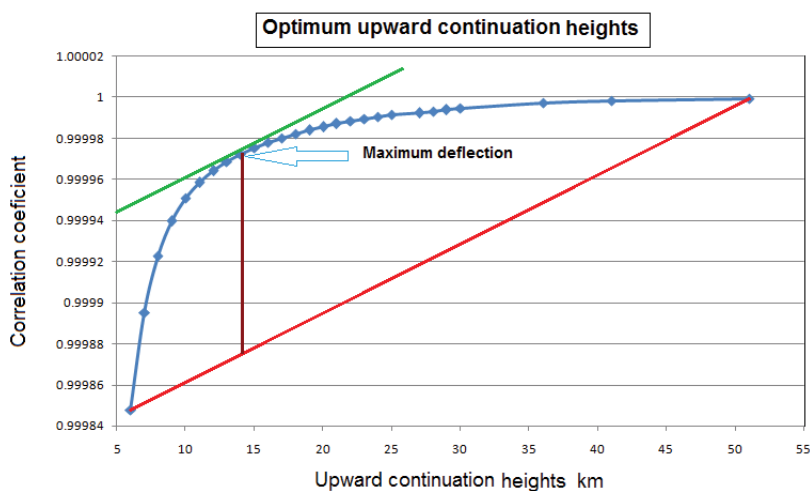
Figure 4: Cross correlations between continuations to two successive upward heights versus the upward heights.

of depositional formations is deduced from the study [19] (Figure 5) shows the locations of the produced profiles in the study area.

Because the modelling software [25] requires straight line profiles, a kriging gridline was calculated for each survey line using all gravity station locations. All stations were projected perpendicularly onto this line, and station distances were calculated from the first station on each line (always the southernmost station).

Residual gravity profiles

Profile G1: This profile extends for about 46 km from southern Ruvia village to the north of Bakirman village (Figure 6). This profile displays two gravity "highs", the first is appeared over the southern Ruvia anticline according to present study with amplitude of about 3.5 mGal and a half-width of approximately 4 km. It may be formed by E-W normal fault. The second is indicated over the northern Ruvia anticline according to present study with amplitude

of about 5 mGal and a half-width of approximately 4 km. It can be explained as a horst bounded by two E-W reverse faults. There are two gravity "lows" in this profile; the first is corresponding with the syncline between southern Ruvia and northern Ruvia anticlines. The second is illustrated above the plunge of Aqra anticline.

Profile G2: This profile extends for about 52 km from Chamma village to Bamishmish village (Figure 7). This profile displays three gravity "highs", the first is shown over the extension of Mandan anticline according to present study with amplitude of about 3 mGal and a half-width of approximately 4 km. The second is illustrated above of northern Ruvia anticline (according to present study) with amplitude of about 10 mGal and a half-width of approximately 4.5 km. The last anomaly is appeared over Aqra anticline with amplitude of about 5 mGal and a half-width of approximately 4.5 km. The two last gravity "highs" over northern Ruvia anticline and Aqra anticline (near Bakirman village) are suggested to be horst
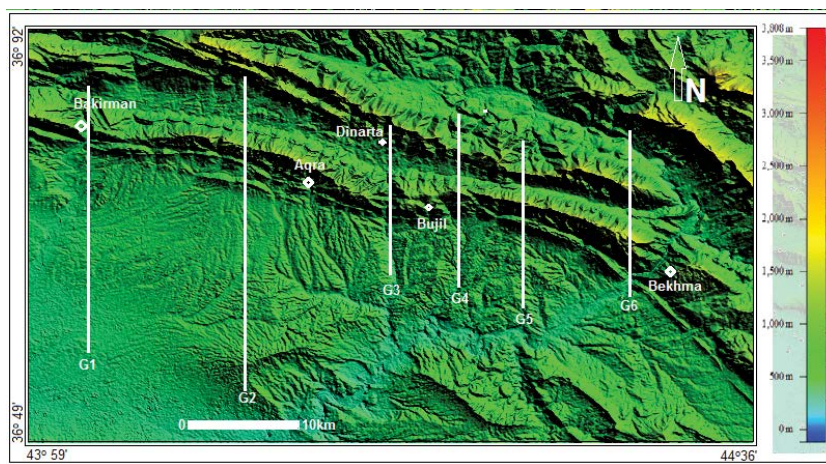
Figure 5: The DEM image with the locations of profiles in the study area
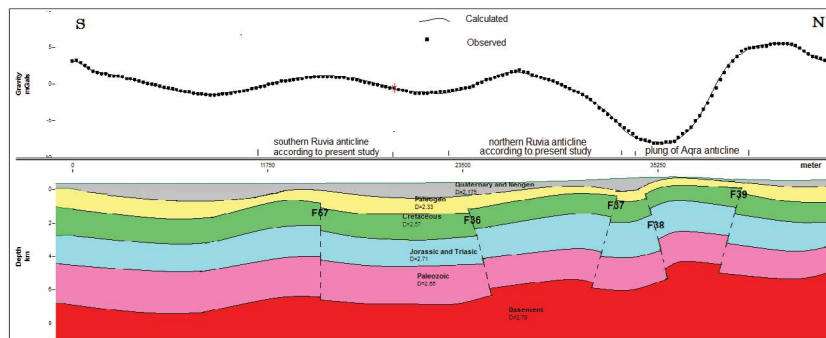
Figure 6: Cross section and gravity data along profile G1. The upper panel shows the gravity profile along the cross section- the dots represent the observed gravity values and the line shows the calculated gravity for the model below. The lower panel shows the modeled geologic cross section- depths are positive downward. F=suggested faults.
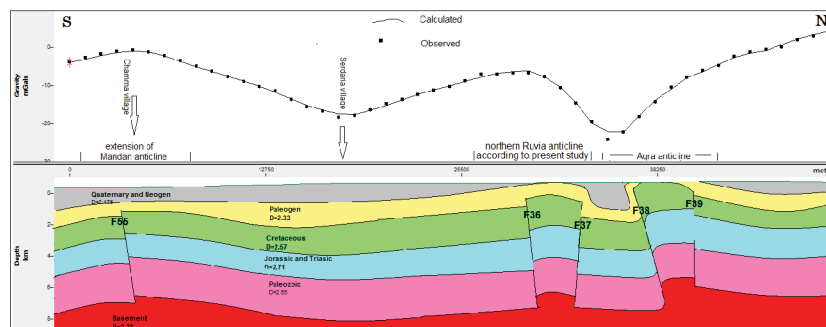
Figure 7: Cross section and gravity data along profile G2. The upper panel shows the gravity profile along the cross section- the dots represent the observed gravity values and the line shows the calculated gravity for the model below. The lower panel shows the modeled geologic cross section- depths are positive downward. F=suggested faults.

bounded with two E-W reverse faults. In addition, there are two synclines in this profile indicated between the previous anticlines.

Profile G3: This profile extends for about 22 km (Figure 8). This profile shows two gravity "highs". The first is indicated over northern Ruvia anticline with amplitude of about 6 mGal and a half-width of approximately 2.5 km. The second is pointed out over Aqra anticline with amplitude of about 4 mGal and a half-width of approximately 2.5 km. Two gravity "lows" are appeared in this profile those located between the anticlines.

Profile G4: This profile extends for about 27 km passing Aqra and Piris anticlines (Figure 9). This profile displays four gravity "highs". The first one is appeared over the northern limb of northern Ruvia anticline. The second one is indicated over the first part of Aqra anticline with amplitude of about 4 mGal and a half-width of approximately 1 km. The third one is pointed out over the second part of Aqra anticline with amplitude of about 12 mGal and a half-width of approximately 3.5 km. The fourth one is seen over the southern limb of Piris anticline. In addition, there are three gravity "lows" in this profile located between the anticlines.

Profile G5: This profile was extended for about 23 km passing northern Ruvia and Piris anticlines (Figure 10). This profile shows two gravity "highs". The first is located over northern Ruvia anticline with amplitude of about 3 mGal and a half-width of approximately 4 km. The second is appeared over the southern limb of Piris anticline. In addition, there is a gravity "low" resulted from the syncline between the northern Ruvia and Piris anticlines.

Profile G6: This profile extends for about 24 km passing Barat anticline and the southern limb of Piris anticline (Figure 11) This profile displays two gravity "highs". The first is located over Barat anticline with amplitude of about 18 mGal and a half-width of

approximately 5 km. This anomaly can be explained as a horst bounded by two NW-SE reverse faults. The second is seen over the southern limb of Piris anticline that may be formed by a reverse fault. In addition, there is one gravity "low" located as a syncline between Barat and Piris anticline.

DISCUSSION

The gravity anomalies in the studied areas reflect the combined effects of Paleozoic, Mesozoic and Cenozoic tectonic development. The faults are matched well with the situation of surface structures described by some authors, and fitting with the information concluded from some local geophysical studies. Basement configuration including basement blocks, major faults were suggested utilizing the gravity profiles. The main gravity lows are attributed to thick low density sediments deposited within grabens which are thrown against the high density sediments by two major E-W, NW-SE faults which give rise to negative density contrast. On the other hand, local anomalies were interpreted to be the reflection of local structures and depressions within the basement and sediments above it.

It is proved that the anticlinal structures which have negative and positive anomalies caused by main deep seated faults associated mostly with shallower faults on the crests of those structures. This conclusion is mismatching with the scenario [34] who postulated that there is only one listric fault underneath each crest of the anticlines.

In addition, it is confirmed that the structures in the present study are not attributed to mainge of lextuer feature [34]. In contrast, it is displayed that the anomalies above those structures are reflected a giant numerous subsurface variations on the boundary of the basement rocks and above it.
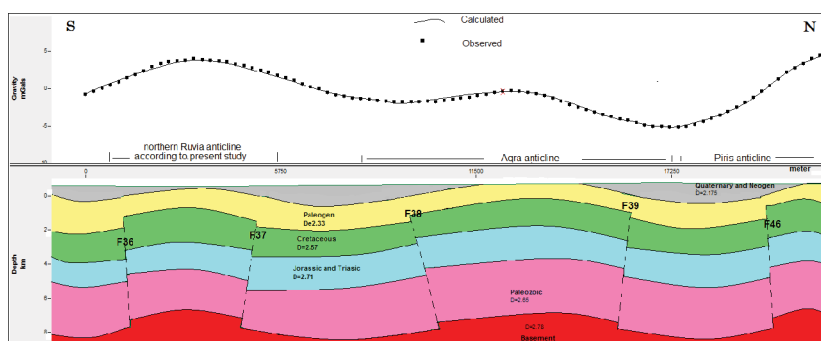
Figure 8: Cross section and gravity data along profile G3. The upper panel shows the gravity profile along the cross section- the dots represent the observed gravity values and the line shows the calculated gravity for the model below. The lower panel shows the modeled geologic cross section-depths are positive downward. F=suggested faults.
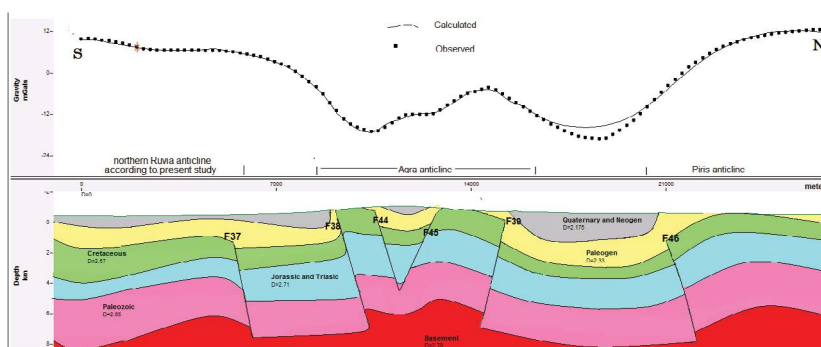
Figure 9: Cross section and gravity data along profile G4. The upper panel shows the gravity profile along the cross section- the dots represent the observed gravity values and the line shows the calculated gravity for the model below. The lower panel shows the modeled geologic cross section- depths are positive downward. F=suggested faults.
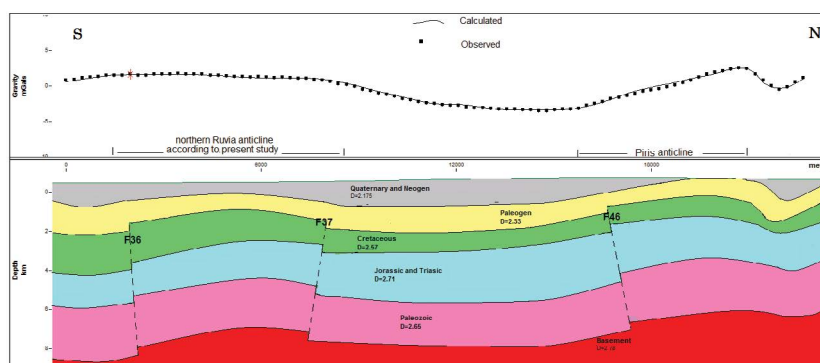
Figure 10: Cross section and gravity data along profile G5. The upper panel shows the gravity profile along the cross section- the dots represent the observed gravity values and the line shows the calculated gravity for the model below. The lower panel shows the modeled geologic cross section- depths are positive downward. F=suggested faults**.**
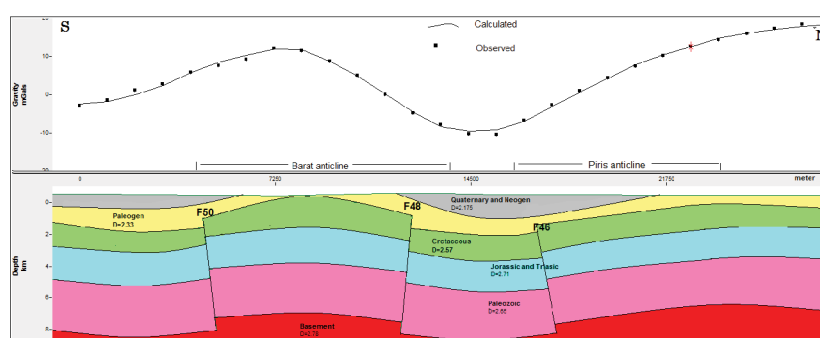
Figure 11: Cross section and gravity data along profile G6. The upper panel shows the gravity profile along the cross section- the dots represent the observed gravity values and the line shows the calculated gravity for the model below. The lower panel shows the modeled geologic cross section- depths are positive downward. F=suggested faults.

The most modelled anomalies in the previous profiles are caused by anticline structures associated with tectonic faults which are formed from grabens and horsts. The following is a discussion of those geophysical anomalies which modeled in the present study.

Northern Ruvia anomaly

It is not clearly appeared on the surface. It is indicated for the first time in the present study as a small positive anomaly with maximum value of about 2 mGal and minimum value of about -1.5 mGal. It can be explained as an anticline formed by a small horst bounded with two E-W reverse faults (F36,F37).

Southern Ruvia anomaly

It is firstly founded out in the present study. It is displayed as a low positive anomaly with maximum amplitude of about 2 mGal and minimum amplitude of about -2 mGal. This anomaly is suggested to be a symmetrical anticline formed by vertical E-W normal fault (F57).

Aqra structure

It is gravity "high" located near Aqra village with maximum value of about-4 mGal and minimum value of about -19 mGal. This anticline appeared as a positive anomaly within bigger negative anomaly same as an anticline within a big syncline. It represents two horsts separated by a graben bounded with two E-W normal faults (F44, F45) that increases the negativity. All observed gravity values over this structure was negative which explains the down lift of this structure and all units under it. In addition, this structure is overturned towards the south that increases the negativity toward it.

Piris structure

It represents a gravity "high" lies at the north of Aqra anticline with maximum value of about 12 mGal and minimum value of about -15 mGal. The southern limb of this structure is indicated as a north end of the big negative anomaly contained Aqra anticline. This negative anomaly can be explained as a big graben bounded by two E-W reverse faults (F37,F46) and the positivity within this graben may be formed by the uplift of Aqra anticline appeared clearly in profile (G2).

Barat structure

It extends along Aqra structure with difference trend NW-SE, that may be explained as an end of the big graben existing over Aqra anticline. It appears as gravity "high" with a maximum value of about 9 mGal and minimum value of about -7 mGal. It is corresponding to a horst bounded with two NW-SE reverse faults (F50, F48). Zagros effect was appeared clearly in this anomaly that changes it's prevailing trend from E-W to NW-SE, which varying the gravity "low" appeared in Aqra anticline (graben) to gravity "high" (horst).

CONCLUSIONS

The following conclusions were reached in the course of this work:

1. During this study, the best separation between the regional and residual anomalies was performed using the new empirical upward continuation method.

2. The optimum upward continuation heights applied to the gravity profiles are ranging between 6.5 and 10 km under sea level that may be reflecting the basement depth which is matching with the 2D models.

3. The present study has concluded a number of new subsurface anticlines as, southern Ruvia and northern Ruvia. In addition, unknown structural extensions are also identified.

REFERENCES

1. Aydogan D, Pinar A, Elmas A, Tarhan Bal O, Yuksel S. Imaging of Subsurface Lineaments in the Southwestern Part of Thrace Basin from Gravity Data. Earth, Planets Space. 2013;65:299-309.

2. Filina I, Delebo N, Mohapatra G, Coble C, Harris G, Layman J, et al. Integration of seismic and gravity data – A case study from the western Gulf of Mexico, Interpretation. 2015;3:99-106.

3. Stadtler C, Fichler C, Hokstad K, Myrlund EA, Wienecke S, Fotland B. Improved salt imaging in a basin context by high resolution potential field data: Nordkapp Basin, Barents Sea. Geophys Prospect. 2014;62:615-630.

4. Hedin P, Malehmir A, Gee DG, Juhlin C, Dyrelius D. 3D interpretation by integrating seismic and potential field data in the vicinity of the proposed COSC-1 drill site, central Swedish Caledonides. Geological Society, London, Special Publications. 2014;390:301-319.

5. Mariita NO. The gravity method, Presented at Short Course II on Surface Exploration for Geothermal Resources, organized by UNU-GTP and KenGen, at Lake Naivasha, Kenya. 2007.

6. Jassim, SZ, Goff JC. Phanerozoic development of the northern Arabian Plate. Geology of Iraq. 2006;32-44.

7. Numan NMS. Basement controls of stratigraphic sequences and structural patterns in Iraq. Geol Soc Iraq J. 1984;16:8-28.

8. Sayyab A, Valek R. Pattern and general properties of the gravity field of Iraq. 23rd Int Geol Cong, Czcechoslovakia. 1968;5:129-142.

9. Al Sinawi SA, Rizkallah RI, Al Rawi FR. On the gravity field of Iraq, Part I, the state of art. J Geol Soc Iraq. 1987;20:17-36.

10. Abbas MJ. Gravity activities in Iraq till the end of year 1983. J Soc Iraq. 1983-1984;16-17:67-87.

11. Hafidh AA. Seismic velocity modeling of north and northeast Iraq using receiver functions, 29th Monitoring Research Review: Ground-Based Nuclear Explosion Monitoring Technologies. 2007.

12. Ghaib FA. Geophysical study of Erbil and Aqra plains and their geological implications. Unp. Ph.D. thesis, University of Salahaddin, Erbil, Iraq. 2001;185.

13. Ghaib FA, Al-Dawoody AN. Reconnaissance Gravity and Magnetic Surveys Across the River Zab West and Northeast Erbil City Iraqi Kurdistan region, University of Salahaddin, Erbil, Iraq. 2010.

14. Døssing A, Hansen TM, Olesen AV, Hopper JR, Funck T. Gravity inversion predicts the nature of the Amundsen Basin and its continental borderlands near Greenland. Earth Planet. Sci. Lett. 2014;408: 132-145.

15. Mutib M. Geophysical investigation around Demir Dagh area, unpub. Msc. thesis, Mosul university, Iraq. 1980.

16. Hamid HI. Reconnaissance gravity traverse between Mosul and Harir plain, N-Iraq, Unpub. M.Sc. Thesis, University of Mosul, Iraq (In Arabic). 1995c.

17. Al-Shaikh ZD, Mohammed ZS. An interpretation of the gravity anomalies over the Tertiary basins of Shaqlawa - Harir area using variable density-depth function. Iraqi Geol J. 1997;30:77-84.

18. Ditmar V, Iraqi-Soviet Team. Geological conditions and hydrocarbon prospects of the Republic of Iraq (northern and central parts) (manuscript report), Iraq National Oil Company, Baghdad, Iraq. 1971.

19. Al-Brifkani MJN. Structural and Tectonic Analysis of the Northern Thrust Zone (East Khabour River) in Iraq, Unpub. Ph.D. thesis, University of Mosul (in Arabic). 2008.

20. Al-Shaikh ZD, Saleh SA, Abdo HF. Contribution to the geology of Shaqlawa - Harir area. Iraqi J. Geo. Soc Special issue. 1975;55-67.

21. Hinze WJ, Aiken C, Brozena J, Coakley B, Dater D, Flanagan G. New standards for reducing gravity data: The North Amer. gravity database. Geophysics. 2005;70:J25-J32.

22. Nabigian ME, Ander VJ, Grauch RO, Hansen TR, Lafehr Y, Li Y, et al. Pearson, Historical Development of the Gravity in Exploration. Geophys. 2005;70:63-89.

23. Hwa Chen K. An Improved Approach for Terrain Correction: Application to Northeast Asia's Highest Peak (Mt. Jade, Taiwan). Sensors. 2009;9:6604-6612.

24. Geosoft (GOM), software for Earth Sciences, Geosoft INC. Toronto, Canada. 2008.

25. Talwani M, Worzel JL, Landisman M. Rapid gravity computations for two dimensional bodies with application to the Mendocino submarine fracture zone. J Geophys Res. 1959;64: 49-59.

26. Talwani M, Heirtzler JR. Computation of magnetic anomalies used by two dimensional bodies of arbitrary shape. in Parks, G. A., Ed., Computers in the mineral industries, Part 1: Stanford Univ. Publ., ecological Sciences. 1964;9:464-480.

27. Won IJ, Bevis M. Computing the gravitational and magnetic anomalies due to a polygon: Algorithms and Fortran subroutines. Geophysics. 1987;52: 232-238.

28. Abbas MJ, Masin J. New geophysical aspects of the basement structure in western Iraq. J. Geol. Soc. Iraq, Special Issue. 1975;1-13.

29. Al-Mashhadani AM. Geophysical evidence for the subsurface structures of the Jezira area, northern Iraq, Unpub. Ph.D. thesis, University of Mosul (in Arabic). 2000.

30. Webring M. SAKI: A Fortran program for generalized linear inversion of gravity and magnetic profiles. USGS Open File Report. 1985;29:85-122.

31. Al-Rahim A. Separating the gravity field of Iraq by using bidimensional empirical mode decomposition technique. Arabian J Geosci. 2016;9:43.

32. Zeng H, Xu D, Tan H. A model study for estimating optimum upward continuation height for gravity separation with application to a Bouguer gravity anomaly over a mineral deposit, Jilin province, northeast china. Geophysics. 2007;72:145–150.

33. Numan NMS. (1997) A plate tectonic scenario for the Phanerozoic succession in Iraq. Iraqi Geol J. 1997;30:2-28.

34. Ameen MS. Regional investigation of geoflexures tectonic analysis in the simple folded zone of Iraq. M.Sc. Thesis, University of Mosul, Iraq. 1979.